





Parameter Tuning of ADRC Controller for Electrode Wire Feed System Using a Fuzzy Algorithm

M. Haddad^{1,*} , B. Babes¹ , N. Hamouda¹ ,
B. Lekouaghet¹ , H. Amar¹ 

¹ Research Center in Industrial Technologies CRTI
P.O. Box 64, Cheraga 16014, Algiers, Algeria
{m.haddad,b.babes,n.hamouda,b.lekouaghet,h.amar}@crti.dz
* Corresponding author

Abstract. This study introduces a method for enhancing the performance of electrode wire feeding mechanisms (EWFMs) in power-controlled arc welding machines. The method uses a fuzzy algorithm to implement an active disturbance rejection controller (ADRC) with self-tuning parameters. A testing system, operating in real-time and built on the dSPACE platform, is set up to verify the proposed method. Initially, the study develops an active disturbance rejection control approach to improve tracking performance and robustness in the presence of multiple disturbances in welding EWFm operations. Subsequently, a fuzzy algorithm-based method is employed to tune the parameters of the ADRC controller, ensuring accurate adjustment of gains. Finally, real-time tests are conducted to validate the effectiveness of the proposed strategy. The results indicate that the ADRC controller with Fuzzy algorithm-based gains tuning exhibits notable capabilities in rejecting disturbances, minimizing overshoot, achieving rapid response, and ensuring high precision.

Keywords: Electrode wire feed mechanism (EWFm), Fuzzy algorithm, welding, Active disturbance rejection control (ADRC), Extended state observer (ESO).

1 Introduction

Arc welding is a fabrication technique employed to fuse metals by subjecting them to the intense heat of an electric arc until they reach their melting points. The feed capacity of the welding wire through the wire liner emerges as the most significant factor affecting arc-welding operations. For instance, when using aluminium electrodes, even a slight deviation of up to 1% in wire feed rate can lead to inconsistent arc lengths, variations in voltage and current, and a deterioration in the weld quality [1]. Consequently, this study proposes a method for enhancing the performance of EWFMs within power-controlled arc-welding machines. The method involves implementing an active disturbance rejection controller (ADRC) with parameters self-tuning using a fuzzy algorithm. A testing system, operating in real-time and built on the dSPACE platform, is established to verify the proposed method. Initially, the

© The Author(s) 2024

C. A. Kerrache et al. (eds.), *Proceedings of the International Conference on Emerging Intelligent Systems for Sustainable Development (ICEIS 2024)*, Advances in Intelligent Systems Research 184,

https://doi.org/10.2991/978-94-6463-496-9_13

study develops an active disturbance rejection control approach to improve tracking performance and robustness in the presence of multiple disturbances in welding EWFM operations. Subsequently, a fuzzy algorithm-based method is employed to tune the parameters of the ADRC controller, ensuring accurate adjustment of gains. Finally, real-time tests are conducted to validate the effectiveness of the proposed strategy. The results indicate that the ADRC controller with Fuzzy algorithm-based gains tuning exhibits notable capabilities in rejecting disturbances, minimizing overshoot, achieving rapid response, and ensuring high precision. To ensure optimal welding outcomes, it is imperative to continuously regulate the wire feed speed (WFS) throughout the arc welding process. Recently, significant efforts have been devoted to developing specialized mechanisms capable of precisely controlling welding WFS variations, spanning from 0.1% to 1.0% of the intended value, throughout welding procedures [2-4].

However, within a range of 60 *m* between the base metal and the wire reel, these specialised mechanisms facilitate controlled feeding. However, choosing such architectures is a more expensive and time-consuming alternative compared to microprocessor-based wire delivery systems. This scenario opens up the possibility of investigating more economical and practical options. The main goals of the digital control of the arc welding process are to guarantee precise and steady WFS and lessen disturbances' effect on the EWFM. Several regulators have been proposed in the literature to control the welding EWFM, including the Proportional-Integral-Derivative (PID) regulator [5], Optimal Tuning of Fractional Order (FO) PID controller [6], Sliding Mode Control (SMC) [7], PSO-Fuzzy-PD μ +I controller [8], and FO-Fuzzy PID controller [9]. Despite their simplicity, the Proportional-Integral-Derivative and Synergetic regulators [10] prove ineffective for managing the disturbed nonlinear EWFM. Conversely, chattering phenomena in SM regulator digital applications will result in high-frequency unmodeled dynamics, which is not desired for welding EWFM control. Consequently, in order to solve the control issue of welding EWFMs, a novel and effective control method is needed.

Typically, the electrode wire feed mechanism regulator is designed to obtain accurate and dependable tracking of the required wire feed velocity across various conditions, ranging from complete to no-load scenarios. However, during these operations, the welding EWFM may encounter significant uncertainties. In such instances, it is believed that the ADRC controller could achieve accurate and constant tracking.

Hence, this article employs an ADRC controller to fulfil the design objectives with maximum accuracy. The design methodology for the active disturbance rejection controller follows the principles of aggregated regulator methods. The active disturbance rejection controller has garnered attention due to its minimal requirement for understanding the regulated system, its adeptness in rejecting disturbances, its simplicity in construction and implementation into actual systems, and its encouraging outcomes.

The key idea behind the active disturbance rejection controller is the instantaneous calculation of overall disturbance, which is the sum of external and internal disturbances through the utilization of an ESO. The anticipated overall disturbance is then immediately ignored by the regulator. The intricate and unpredictable dynamics of the

plant are simplified into a cascaded integrated plant, which can be easily controlled using a PD regulator due to its ability to reject disturbances. An ADRC controller has three main characteristics: it only relies on two adjustment factors, namely the observer bandwidth and the regulator bandwidth, and it demands little knowledge of the system's model. It also has a high ability to reject disturbances. The ADRC controller may be seen as a model-free regulator. Many industries have used the ADRC controller [11-15]. This regular offer accuracy, minimal overshoot, fast reaction times, and efficient disturbance rejection. However, the conventional ADRC limits its practical application, making the control mechanism and parameter adjustment more difficult. Thus, it is imperative to create an effective and efficient system to improve the advantage of the standard ADRC controller.

This study explores gain adjustment methods, focusing on the fuzzy algorithm, to enhance the ADRC controller's ability to reject disturbances and improve stabilization accuracy in welding EWF. Certain gains in the ADRC controller are optimized and determined, mitigating the challenges associated with manual adjustment and preventing any potential blind adjustments. Moreover, laboratory experiments are carried out to authenticate the suggested methodology.

2 Welding EWF Topologies

The conventional metal welding technique uses heat from an electric arc to melt the material for welding. The GMAW (Gas Metal Arc Welding) process utilizes this principle and includes a shielding gas. The wire feed velocity of the EWF ranges from 150 to 1800 cm/min, depending on the wire diameter. The GMAW system consists of a gearbox, feed rollers, a 24V DC motor, and a guide tube clamp, which can be mounted inside the welding power source cabinet or as a standalone unit. The fundamental configuration of GMAW machines is illustrated in Fig. 1. Proper configuration of the GMAW equipment ensures a smooth wire feeding and arcing sequence, resulting in solid welds.

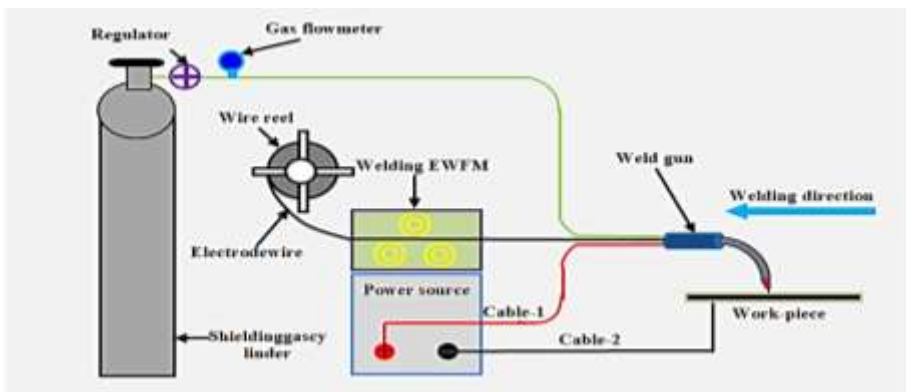


Fig. 1. Configuration of the GMAW system.

The servomotor operates based on the electromechanical wire feed system depicted in Fig. 2.

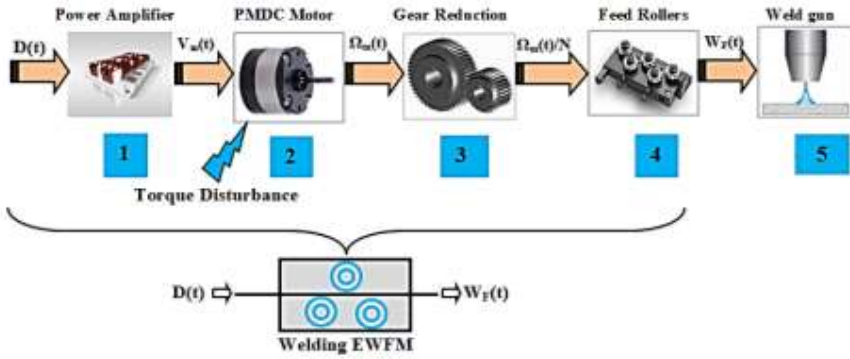


Fig. 2. Servomotor-driven EWFM welding.

The system's control input is assumed to be the duty cycle $D(t)$, which powers the permanent magnet DC (PMDC) motor through power amplification. The PMDC motor drives a series of pinch rollers through a reduction gearbox. The output signal $\Omega_m(t)$ describes the voltage of a rotary encoder connected to a PMDC motor. Adequately scaled, this signal provides a sampling of the wire feed rate $W_F(t)$ in (cm/min). The torque disturbance in the welding EWFM results from friction within the wire-feeding channel and the eccentricity of the wire-wrapping apparatus.

3 Welding EWFM MODELING

Eqs. (1)-(4) form the theoretical framework for characterizing the mathematical model of welding EWFM. They encompass the electromechanical conversion, background electromagnetic field, rotating circuit voltage, and mechanical formulas.

$$\Gamma_m = K_m \cdot I_m \quad (1)$$

$$U_m = K_e \cdot \Omega_m \quad (2)$$

$$V_m = R_m \cdot I_m + L_m \cdot \frac{dI_m}{dt} + U_m \quad (3)$$

$$\Gamma_m = J \cdot \frac{d\Omega_m}{dt} + \Gamma_L + \Gamma_h + \Gamma_\Omega \quad (4)$$

where Ω_m represents the angular displacement that an unknown torque perturbation input might impact, I_m denotes the armature current, and V_m is the input voltage that is considered the control input. Γ_h and Γ_Ω represent a nonlinear model of dry friction, Γ_L denotes the load torque, and J signifies the moment of inertia. Γ_m and R_m represent the armature's inductance and resistance, while K_m and K_e stand as constants.

The paragraph suggests combining Eqs. (1)-(4) to derive equations describing the dynamics of the EWFM by ignoring the PMDC inductor.

$$\frac{d\theta_m}{dt^2} = \frac{V_m.K_m}{J.R_m} - \frac{\Gamma_L}{J} - \frac{\Gamma_h}{J} - \frac{\Gamma_\Omega}{J} - \frac{K_e.K_m}{J.R_m} \cdot \frac{d\theta_m}{dt} \quad (5)$$

To get the equation of state for the welding EWFM, we may use Eq. (5) in the following manner:

$$\begin{cases} \dot{x}_1 = x_2 \\ \dot{x}_2 = x_3 + b.V_m \\ \dot{x}_3 = \dot{d} \\ y = x_1 \end{cases} \quad (6)$$

where $x_1 = \theta_m$, $x_2 = \Omega_m = \frac{d\theta_m}{dt}$, $d = -\frac{K_e.K_m}{J.R_m} \cdot x_2 - \frac{\Gamma_L}{J} - \frac{\Gamma_h}{J} - \frac{\Gamma_\Omega}{J}$, and $b = \frac{K_m}{J.R_m}$.

The symbol θ_m represents the output angle of the PMDC motor shaft. The variable b is a constant value. The symbol d represents the generalized disturbance, which includes total disturbances and unidentified system dynamics. The ADRC controller may be designed to control the WFS by utilizing the state space model of the EWFM, as described in Eq. (6).

It is challenging to control the wire feed velocity in EWFM welding due to its multiplicative nonlinearity and external torque disturbances. To address these challenges, an ADRC controller was utilized in this study to effectively counteract all forms of disturbances, such as external disturbances and nonlinearity within the welding procedure. The ADRC controller achieves this by extracting and compensating for the complete disturbance utilizing an ESO. Furthermore, the adjustment of regulator gains using a fuzzy algorithm is explored in this article. The objective is to ensure that the wire feed velocity (W_F) closely follows a specified reference trajectory (W_F^*) for the motor shaft angular speed, achieved through a control law represented by $\tau = V_m$.

4 ADRC Controller

The ADRC controller offers a different approach by blending the features of a traditional PID controller with contemporary model-based methods [15]. It consists of three key elements:

1. The Nonlinear Tracking Differentiator (NTD),
2. The Extended State Observer (ESO), and
3. The Nonlinear State Error Feedback (NLSEF).

This integrated approach aims to effectively tackle control issues in diverse, dynamic systems [15].

4.1 NTD algorithm

The NTD ensures the input progresses seamlessly without exceeding its maximum, extracts a continuously different signal for non-differentiable reference inputs of the system, and rapidly follows the reference input $v_0(k)$. The equation for the discretized Nonlinear Time-Delay (NTD) is represented by Eq. (7):

$$\begin{cases} v_1(k+1) = v_1(k) + \mu v_2(k) \\ v_2(k+1) = v_2(k) + \mu \tau(k), \quad |\tau(k)| \leq r \end{cases} \quad (7)$$

where

$$\tau(k) = fhan(v_2(k) - v_0(k), v_2(k), r, \mu) \quad (8)$$

In Eq. (7), $v_1(k)$ represents the tracked value of $v_0(k)$, while $v_2(k)$ indicates the differential tracking value of $v_0(k)$. Parameters r and μ act as regulators, and $fhan(v_2(k) - v_0(k), v_2(k), r, \mu)$ denotes a nonlinear function. The formulation of this expression is as follows:

$$\begin{cases} d = d_0 r^2, a_0 = \mu v_2(k), y(k) = v_1(k) + a_0 \\ a_1 = \sqrt{d(d + 8|y(k)|)} \\ a_2 = a_0 + \text{sign}(y(k))(a_1 - d)/2 \\ s_y = (\text{sign}(y(k) + d) - \text{sign}(y(k) - d))/2 \\ a = (a_0 + y(k) - a_2)s_y + a_2 \\ s_a = (\text{sign}(a + d) - \text{sign}(a - d))/2 \\ fhan = -r \left(\frac{a}{d} - \text{sign}(a) \right) s_a - r \text{sign}(a) \end{cases} \quad (9)$$

The above equation produces two signals, $v_1(k)$ and $v_2(k)$, based on a specific reference input. These signals are employed to monitor the reference input, $v_0(k)$, and its corresponding differential signal.

4.2 ESO algorithm

The ESO monitors the general disruption $d(k)$ and eliminates it using the NLSEF algorithm to mitigate the disturbance successfully. Therefore, the effect of the welding EWFM on the disturbance is determined by the regulator output through a nonlinear ESO and can be expressed by Eq. (10).

$$\begin{cases} e(k) = Z_1(k) - y(k) \\ fe = fal(e, r, \mu) \\ fe_1 = fal(e_1, r, \mu) \\ Z_1(k+1) = Z_1(k) + \mu(Z_2(k) - \theta_1 e(k)) \\ Z_2(k+1) = Z_2(k) + \mu(Z_3(k) + b \tau(k)) - \theta_2 fe \\ Z_3(k+1) = Z_3(k) - \mu \theta_3 fe_1 \end{cases} \quad (10)$$

In Eq. (10), y represents the output of the EWFM. $Z_1(k)$ and $Z_2(k)$ correspondingly stand for the tracking functions for $y(k)$ and its derivative signal. $Z_3(k)$ represents the anticipated variable for combined internal and external disturbances. θ_1 , θ_2 , and θ_3 are adjustable parameters. The factors θ_1 , θ_2 , and θ_3 have the most significant impact on the success of ESO operations. The vibration can be effectively reduced by raising the values of θ_1 and θ_2 . However, if the value is very high, the ADRC controller will exhibit divergence. The variable b_0 denotes the rate of compensation. It is seen that the following relationship exists between the controlled system's bandwidth λ_c and variables θ_1 , θ_2 , and θ_3 :

$$\theta_1 = 3\lambda_c, \theta_2 = 3\lambda_c^2, \theta_3 = \lambda_c^3 \quad (11)$$

The function $fal(e, \alpha, \mu)$ is given by:

$$fal(e, \alpha, \mu) = \begin{cases} \frac{e}{\mu^{1-a}}, & |e| \leq \mu \\ |e|^\alpha sign(e), & |e| > \mu \end{cases} \quad (12)$$

where a ranging from 0 to 1 determines the tracking velocity, while μ , a positive factor, affects the filtering process. The fal function is highly sensitive to small mistakes and lowly sensitive to significant errors.

4.3 NLSEF algorithm

The NLESF method integrates the error signal and its derivative through a non-linear process, including disturbance correction, to modify the measured control variable and produce the final control variable.

$$e_1(k+1) = v_1(k+1) - Z_1(k+1) \quad (13)$$

$$e_2(k+1) = v_2(k+1) - Z_2(k+1) \quad (14)$$

$$\tau_0(k+1) = \rho_1 fal(e_1(k+1), \alpha, \delta) + \rho_2 fal(e_2(k+1), \alpha, \delta), \quad (15)$$

$$0 < \rho_1 < 1 < \rho_2$$

$$\tau(k+1) = \tau_0(k+1) - \frac{Z_3(k+1)}{b_0} \quad (16)$$

where e_1 and e_2 represent the tracking state errors, while ρ_1 and ρ_2 denote the parameters requiring tuning.

The overall setup of the WFS control framework based on ADRC can be structured as depicted in Fig. 3.

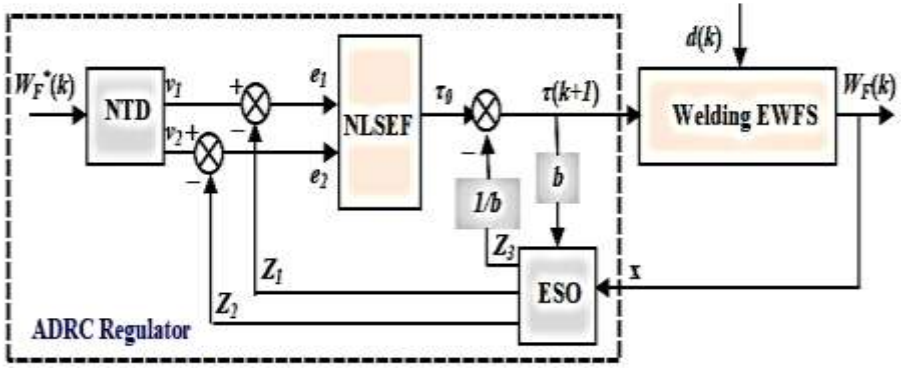


Fig. 3. General structure of the wire feed rate control system based on ADRC.

The ADRC controller consists of three main components:

1. The NTD block retrieves the reference signal from the desired WFS W_F^* . It orchestrates the transition response process of W_F , balancing overshoot and response time interaction.
2. The ESO block calculates the actual disturbance value $d(t)$ and utilizes feedback compensation to mitigate its impact. This enhances the ADRC controller's capability to handle disturbances effectively.
3. The NLSEF block calculates the control law $\tau(k + 1)$ using the output signal deviation from the NTD and ESO blocks.

The primary aim of the upcoming section is to optimize the ADRC controller, ensuring stabilization of the WFS while swiftly reducing error to zero.

4.4 Fuzzy-ADRC controller

In assessing the efficacy of the developed Fuzzy-ADRC controller, which employs a fuzzy algorithm to enhance the conventional ADRC controller [16], we consider the scenario where the fuzzy method takes the state errors e_1 and e_2 as inputs and produces K_1 and K_2 as adjusted factors for ρ_1 and ρ_2 , respectively.

$$\begin{cases} \rho_1' = K_1 \rho_1 \\ \rho_2' = K_2 \rho_2 \end{cases} \quad (17)$$

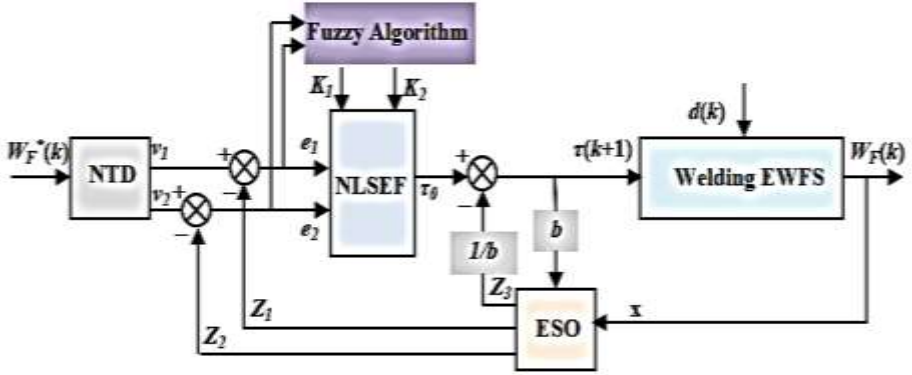


Fig. 4. Structure of fuzzy-ADRC gains self-tuning controller.

In general, the fuzzy method can be simplified into three primary parts:

1. *Fuzzification*

The fuzzy approach involves four variables: e_1 , e_2 , K_1 , and K_2 . Each input (e_1, e_2) and output (K_1, K_2) has triangular Membership Functions (MFs), with seven language groups encompassed in each domain. The domains of e_1 and e_2 range from -1 to 1 , while K_1 and K_2 span from -0.1 to 0.1 . These language groups include Negative Large (NL), Zero (Z), Negative Medium (NM), Positive Small (PS), Negative Small (NS), Positive Medium (PM), and PB (Positive Big), each within its respective domain. Output and input gains are fuzzified, with Fig. 5 illustrating the associated MFs.

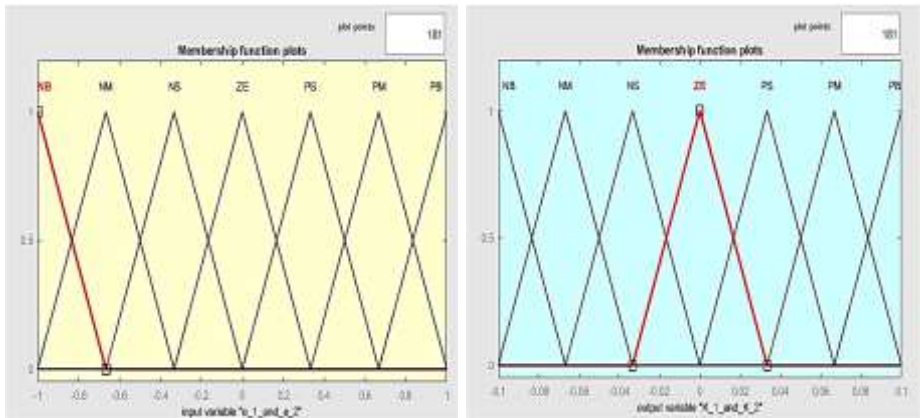


Fig. 5. MFs of the state-errors e_1, e_2 , and the gains K_1 and K_2 .

2. Fuzzy logic reasoning

This study employed Madmen's fuzzy reasoning approach, wherein the gains ρ_1 and ρ_2 of the NLSEF block are dynamically adapted online through the error reduction method. The fuzzy's rules were concurrently formulated, as depicted in Tables 1 and 2.

Table 1. The K_1 gain's fuzzy rules.

K_1	e_2							
	NL	NM	NS	Z	PS	PM	PB	
e_1	NL	PB	PB	PM	PM	PS	Z	Z
	NM	PB	PB	PM	PS	PS	Z	NS
	NS	PM	PM	PM	PS	Z	NS	NS
	Z	PM	PM	PS	Z	NS	NM	NM
	PS	PS	PS	Z	NS	NS	NM	NM
	PM	PS	Z	NS	NM	NM	NM	NL
	PB	Z	Z	NM	NM	NM	NL	NL

Table 2. The K_2 gain's fuzzy rules.

K_2	e_2							
	NL	NM	NS	Z	PS	PM	PB	
e_2	NL	PS	NS	NL	NL	NL	NM	PS
	NM	PS	NS	NL	NM	NM	NS	Z
	NS	Z	NS	NM	NM	NS	NS	Z
	Z	Z	NS	NS	NS	NS	NS	Z
	PS	Z	Z	Z	Z	Z	Z	Z
	PM	PB	NS	PS	PS	PS	PS	PB
	PB	PB	PM	PM	PM	PS	PS	PB

3. Defuzzification

The output value is determined by calculating the weighted average of the MFs. The defuzzification procedure is then performed employing the area centre of gravity method. The fuzzy algorithm continuously adjusts the control values ρ_1 and ρ_2 in real-time. The key parameters have been identified utilizing the fuzzy-ADRC controller, as depicted in Table 3.

Table 3. Fuzzy-ADRC controller gain values.

Regulator	Gain				
	θ_1	θ_2	θ_3	μ	α
Fuzzy-ADRC	59	1214	8000	0.0175	3.75

5 Experimental Verification

Several tests were undertaken to evaluate the efficacy of the optimized Fuzzy-ADRC controller. The welding wire used in this investigation was a copper-coated coil weighing 15 kg and having a diameter of 1 mm. The wire was classified as AWS ER70S-6. The dSPACE controller panel was utilized to implement the WFS regulator for welding EWF. A 200W PMDC motor served as a servomotor, accompanied by a 1000 lines/rev encoder to gauge WFS. Control over the PMDC motor was maintained using an ARBF-ADRC regulator, operating at a sampling frequency of 50 MHz. The Fuzzy-ADRC controller was implemented on a computer and connected to the dSPACE digitally to transmit the WFS feedback data. Refer to Fig. 6 for a schematic representation of the laboratory setup.



Fig. 6. Laboratory test bench.

A PMDC motor is part of the experimental setup, as shown in Fig. 6. The parameters of the PMDC motor employed in this case study are outlined in Table 4.

Table 4. Servo system's specifications.

Parameters / Indication	Value / Unit
Reduction ratio (N)	280.576
Speed Coefficient (K_e)	450 rpm/V
Frictional Moment Coefficient (K_f)	1.204 N.m/rad
Torque Coefficient (K_m)	20.5 mN.m/A
Motor Resistance (R_m)	0.75 Ohm
Moment of Inertia (J)	30.25 g.cm ²
Motor Inductance (L_m)	0.150 mH

Multiple tests have been carried out using sine-wave, step-wave, and triangular-wave signal responses to assess and demonstrate the advantages of the fuzzy-ADRC controller. Figs. 7-8-9 illustrates the control performance of WFS (W_F) and PMDC current (I_m) influenced by the ADRC controllers.

5.1 EWFM's dynamic performance with step-wave signal responses

Fig. 7 depicts the step-wave signal responses of the used controller, showcasing its superior response WFS and robustness performance. Fig. 7 illustrates the suggested regulator's remarkable ability to track wire speed effectively, even with unknown perturbations.

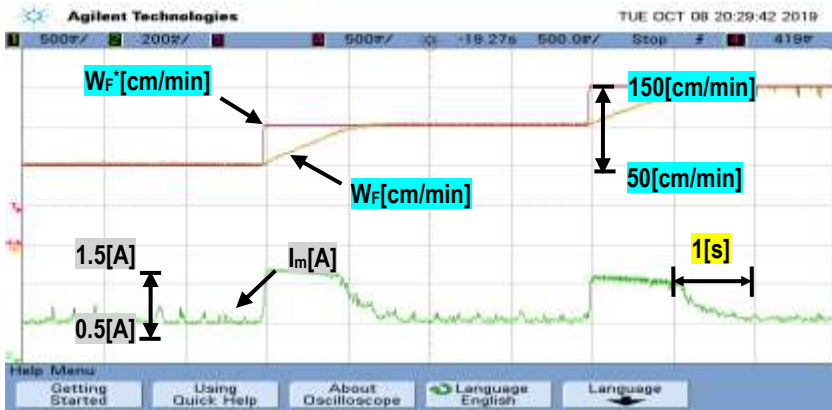


Fig. 7. Step-wave signal responses.

5.2 EWFM's dynamic performance with triangular-wave signal responses

To provide additional evidence of the proposed fuzzy-ADRC controller's effectiveness, we modify the required wire feed velocity signal to a triangular wave, as depicted in Fig. 8. This figure illustrates that the suggested fuzzy-ADRC controller exhibits excellent performance tracking WFS and guarantees zero steady-state error (e_{ss}) in wire feed velocity.

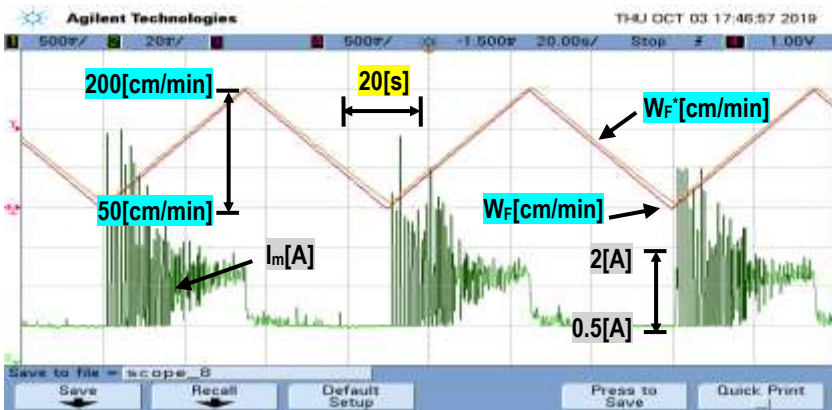


Fig. 8. Triangular-wave signal responses.

5.3 EWFM's dynamic performance when subjected to sine-wave signal responses

Experimental tests were conducted to confirm the effectiveness of the Fuzzy-ADRC controller in minimizing oscillations (Fig. 9) in response to sine-wave signals.

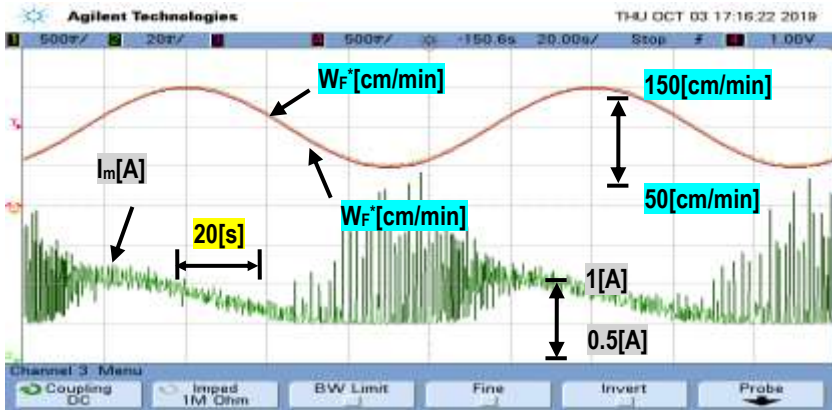


Fig. 9. Sine-wave signal responses.

6 Conclusion

This study concentrated on improving the effectiveness of the ADRC controller in managing the WFS of welding EWFM by employing an online optimization algorithm. The Fuzzy-ADRC combo was suggested to attain enhanced reaction speed and improved electrode wire speed tracking performance. Experimental tests were conducted to confirm the effectiveness and efficiency of the Fuzzy-ADRC controller. These tests involved applying step, triangular, and sine-wave signals to assess the robustness of the proposed ADRC controller. In summary, the experimental tests consistently demonstrate the superior performance of the introduced ADRC controller. According to the experimental findings, the Fuzzy-ADRC controller enhances the EWFM's capacity to handle various disturbances like nonlinearity and load fluctuations while improving tracking accuracy and resilience against significant changes in torque load. For future work, a comparative study with other advanced control algorithms could be conducted to further validate and benchmark the performance of the Fuzzy-ADRC controller.

References

1. Quinn, T.P.: Process sensitivity of GMAW: aluminum vs. steel. *Welding Journal* **81**(4), 554-60s (2002)
2. Samokovliisky, D.A.: Wire feed systems for robotic MIG welding. *Metal Construction* **18**(5), 293-296 (1986)

3. Kuvin, B.F.: New wire feeders ready to deliver the goods. *Welding Design and Fabrication (USA)* **71**(2), 29-32 (1998)
4. Almy, D.: Wire-feed upgrade drives aluminum-welding productivity. *Metal Forming*, **34**(4), 28-32 (2000)
5. Chaouch, S., Hasni, M., Boutaghane, A., Babes, B., Mezaache, M., Slimane, S., & Djenaihi, M.: DC-motor control using arduino-uno board for wire-feed system. In: 2018 International Conference on Electrical Sciences and Technologies in Maghreb (CISTEM), pp. 1-6. IEEE, October 2018
6. Hamouda, N., Babes, B., Hamouda, C., Kahla, S., Ellinger, T., & Petzoldt, J.: Optimal tuning of fractional order proportional-integral-derivative controller for wire feeder system using ant colony optimization. *Journal Européen des Systèmes Automatisés* **53**(2), 157-166 (2020)
7. Paul, A.K.: Experimental design approach to explore suitability of PI and SMC concepts for power electronic product development. *Int. J. Power Electron.* **6**(1), 42-65 (2014)
8. Hamouda, N., Babes, B., Kahla, S., HAMOUDA, C., & Boutaghane, A.: Particle Swarm Optimization of Fuzzy Fractional PD μ + I Controller of a PMDC Motor for Reliable Operation of Wire-Feeder Units of GMAW Welding Machine. *PRZEGL? D ELEKTROTECHNICZNY* **48**(12), 40-46 (2020)
9. Babes, B., Albalawi, F., Hamouda, N., Kahla, S., & Ghoneim, S.S.: Fractional-fuzzy PID control approach of photovoltaic-wire feeder system (PV-WFS): Simulation and HIL-based experimental investigation. *IEEE Access* **9**, 159933-159954 (2021)
10. Hamouda, N., Babes, B., Boutaghane, A.: Design and Analysis of Robust Nonlinear Synergetic Controller for a PMDC Motor Driven Wire-Feeder System (WFS). In: Bououden, S., Chadli, M., Ziani, S., Zelinka, I. (eds) *Proceedings of the 4th International Conference on Electrical Engineering and Control Applications. ICEECA 2019. Lecture Notes in Electrical Engineering*, vol 682. Springer, Singapore (2021).
11. Zhao, S., Usher, N., Morris, D., & Vincent, J.: Fixed-point implementation of active disturbance rejection control for superconducting radio frequency cavities. In: 2013 American Control Conference (ACC), pp. 2693-2698. IEEE, June 2013
12. Zheng, Q., & Gao, Z.: Predictive active disturbance rejection control for processes with delay. In: *Proceedings of the 32nd Chinese Control Conference (CCC)*, pp. 4108-4113. IEEE, July 2013
13. Zheng, Q., Dong, L., Lee, D.H., & Gao, Z.: Active disturbance rejection control for MEMS gyroscopes. In: 2008 American Control Conference (ACC), pp. 4425-4430. IEEE, June 2008
14. Babes, B., Boutaghane, A., Reddaf, A. et al. An RBF neural network-based parameter tuning for an ADRC regulator of electrode wire feed mechanism: arc welding applications. *Weld World* **68**, 987-999 (2024). <https://doi.org/10.1007/s40194-024-01742-4>.
15. Wang, Z., Liu, S., He, K., Shi, W., & Chen, S.: Design decoupling controller for rewinding system of the gravure printing machines. In: 2020 IEEE 5th Information Technology and Mechatronics Engineering Conference (ITOEC), pp. 908-912. IEEE, June 2020
16. Bo, Q., Wang, P., Chai, X., Gong, Y., Li, X., Li, T., Liu, H., & Wang, Y.: Mirror milling trajectory planning for large thin-walled parts based on Fuzzy-ADRC controlled force pre-supporting. *Journal of Manufacturing Processes* **85**, 192-204. (2023).

Open Access This chapter is licensed under the terms of the Creative Commons Attribution-NonCommercial 4.0 International License (<http://creativecommons.org/licenses/by-nc/4.0/>), which permits any noncommercial use, sharing, adaptation, distribution and reproduction in any medium or format, as long as you give appropriate credit to the original author(s) and the source, provide a link to the Creative Commons license and indicate if changes were made.

The images or other third party material in this chapter are included in the chapter's Creative Commons license, unless indicated otherwise in a credit line to the material. If material is not included in the chapter's Creative Commons license and your intended use is not permitted by statutory regulation or exceeds the permitted use, you will need to obtain permission directly from the copyright holder.

